MODEL REDUCTION AND CONTROL IN REACTOR–HEAT EXCHANGER NETWORKS

Michael Bâldea * **Prodromos Daoutidis** *

* *Department of Chemical Engineering and Materials Science, University of Minnesota, Minneapolis, MN 55455*
Telephone: (612) 625 8818, email: daoutidi@cems.umn.edu

Abstract: This paper focuses on energetic aspects of the dynamics and control of process networks with high material recycle. Two prototype systems are analyzed, for which the large material recycle acts as an energy carrier, leading to a high energy throughput for the entire network. Using singular perturbation arguments, we show that the variables in the energy balance of these networks evolve in the fast time scale, while the terms in the material balance equations can exhibit both fast and slow transients. We present a procedure for deriving reduced-order, non-stiff models for the fast and slow dynamics, the latter typically of low order, and a framework for rational control system design, that accounts for the time scale separation exhibited by the system dynamics. The theoretical results are illustrated in a reactor-external heat exchanger network example.

Keywords: model reduction, nonlinear control, energy recycle, singular perturbations

1. INTRODUCTION

Integrated process networks, consisting of individual units interconnected through material and energy recycle, are the rule, rather than the exception in the process industries. The dynamics and control of such networks present distinct challenges, since, in addition to the nonlinear behavior of the individual units, the feedback interactions among these units, induced by the recycle, typically give rise to more complex overall network dynamics (*e.g.* (Morud and Skogestad, 1994; Mizsey and Kalmar, 1996; Jacobsen and Berezowski, 1998; Bildea and Dimian, 1998)).

At the same time, the efficient transient operation of such networks is of critical importance, as the current economic environment imposes frequent changes in operating conditions and objectives (*e.g.* changes in product grade and feed switching), requiring tighter coordination of the plant-wide optimization and advanced control levels (Marquardt, 2000; Kulhavy et al., 2000). A major bottleneck towards analyzing, optimizing and improving the control of process networks is the often overwhelming size and complexity of their dynamic models, which make dynamic simulation computationally intensive and the design of fully centralized nonlinear controllers on the basis of entire network models impractical (such controllers are almost invariably difficult to tune, expensive to implement and maintain, and sensitive to measurement errors and noise). Indeed, the majority of studies on control of networks with material (*e.g.* (Luyben, 1993; Yi and Luyben, 1997)) and energy recycle (*e.g.* (Luyben, 1998; Reyes and Luyben, 2000; Chen and Yu, 2003)) are within a multi-loop linear control framework. The strong coupling between the control loops in different process units in a process network has consequently been recognized as a major issue that must be addressed in a plant-wide control setting (Price

[1] Partial support for this work by ACS-PRF, grant 38114-AC9 and NSF-CTS, grant 0234440 is gratefully acknowledged.

and Georgakis, 1993; Luyben et al., 1997; Ng and Stephanopoulos, 1998), and several strategies have been proposed to this end. (Georgakis, 1986) suggested the use of empirically identified extensive fast and slow variables for the synthesis of nonlinear controllers for a process network. Using the concept of passivity, (Farschman et al., 1998; Hangos et al., 1999) introduced a formal framework for stability analysis and stabilization of process networks using distributed control, subject to thermodynamic and equipment constraints. Finally, (Tyreus, 1999) proposes an analysis method for identifying a small number of dominant variables of a network, that are subsequently used in a partial control framework (Kothare et al., 2000).

In our previous work (Kumar and Daoutidis, 2002; Kumar and Daoutidis, 2003), we considered networks and staged processes with high internal flows compared to the throughput. Within the framework of singular perturbations, we established that the large recycle induces a time scale separation, with the dynamics of individual processes evolving in a fast time scale with weak interactions, and the dynamics of the overall system evolving in a slow time scale where these interactions become significant; this slow dynamics is usually nonlinear and of low order. Motivated by this, we proposed a method for deriving nonlinear low-order models of the slow dynamics, and a controller design framework comprising of properly coordinated controllers designed separately in the fast and slow time scales.

In (Baldea et al., 2004), we focused on process networks with recycle, in which small quantities of inert components are present and a small purge stream is used for their removal. Adopting again a singular perturbation perspective, we established the presence of a slow dynamics associated with the inert, derived explicit descriptions of this dynamics and outlined a framework for rationally addressing the control of inert levels in the network.

In the present paper we focus on the energetic aspects of process networks with high material recycle. We analyze two prototype systems for which the large material recycle acts as an energy carrier, leading to a high energy throughput for the entire network. First, we consider the case of a reactor where a highly exothermic set of reactions takes place, interconnected with an external heat exchanger through a large material recycle stream for more effective heat removal. Using singular perturbation arguments, we show that the dynamics of such networks typically exhibit two time scales, with the energy dynamics evolving in the fast time scale, and the material balance dynamics of the entire network evolving in the slow time scale. We describe a method for deriving approximate, non–stiff, reduced–order models for the dynamics in each time scale, and propose a controller design framework that accounts for this time scale separation. Subsequently, we turn our attention to high purity distillation with large internal recycle, and show that the energy throughput in the column is also high. We also show that the energy dynamics of the column are fast, while the variables related to the material balance exhibit both fast and slow transients in their evolution, and, finally, we outline a procedure for deriving reduced-order, non-stiff, nonlinear models for the fast and slow dynamics of the column.

Throughout our derivations, we use the standard order of magnitude notation $\mathcal{O}(.)$.

2. DYNAMICS OF REACTOR–EXTERNAL HEAT EXCHANGER NETWORKS

In processes in which reactions with significant thermal effects are present, adiabatic reactor operation is not possible and direct heating/cooling for isothermal operation is often impractical or infeasible. In such cases, large material recycle streams are frequently used as heat carriers, connecting the reaction unit to an external heat exchange system (Seider et al., 1999). This configuration allows for more efficient heat exchange, due to the high flowrates of the recycle and the heating/cooling medium. The efficiency of the external heat exchanger can be increased further by increasing the heat capacity of the recycle stream, either by using excess quantities of a reactant or by introducing an inert diluent in the recycle loop, along with a separation unit. Such configurations can be used in both batch and continuous processes, and are quite common in processes featuring fast, highly exothermic reactions (*e.g.* polymerization).

Existing literature on the control of reactor–external heat exchanger networks is relatively scarce, concerning mostly the implementation of linear (Alhumaizi, 2000; Henderson and Cornejo, 1989) and nonlinear (Dadebo et al., 1997) control structures on specific processes. These studies report several control challenges, including difficult tuning of PID and model–based controllers due to the ill–conditioning of the process model.

2.1 *Modeling of Reactor–External Heat Exchanger Networks*

We consider a process network, comprising of a reactor and a heat exchanger. For the case in which an inert heat transfer medium is used, a unit separating the medium from the reaction mass could also be considered. Let M denote the reactor holdup, M_R the holdup in the tube side of the heat exchanger and M_C the holdup in the shell side. Let F_o be the

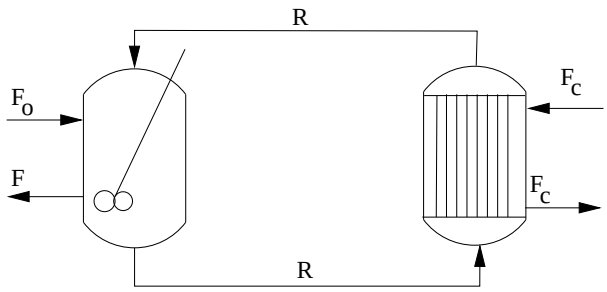

Fig. 1. Schematic diagram of a process network with external heat exchanger

feed flowrate to the reactor, F the effluent flowrate from the network, F_c the coolant flowrate and R the recycle flowrate. Let T_o be the temperature of the feed stream, T the reactor temperature, T_R the temperature of the reaction mass in the tube-side of the heat exchanger, T_{co} and T_c the inlet and outlet temperature of the cooling medium, respectively. $\mathcal{C}$ components are present in the network and participate in $\mathcal{R}$ stoichiometrically independent reactions, with reaction rate $r_i, i = 1, \ldots, \mathcal{R}$ and stoichiometric matrix $\underline{\underline{S}} \in \mathbb{R}^{\mathcal{C}\times\mathcal{R}}$. We denote the heat of reaction vector by $\underline{\Delta H} = [\Delta H_1, \ldots, \Delta H_{\mathcal{R}}]^T$. We assume that the thermal effect of the reactions is very high and that the adiabatic operation of the reactor is not possible. In order to control the reactor temperature, the reaction mass is recycled at a high rate (compared to the feed) through the heat exchanger. For simplicity, we consider the density and heat capacity of the reactants and products (ρ and C_p) and of the cooling medium used in the heat exchanger (ρ_c and C_{pc}) to be constant, and C_p and C_{pc} to be of comparable magnitude, *i.e.* $C_p/C_{pc} = k_{cp} = \mathcal{O}(1)$. Assuming that all units are modeled as lumped parameter systems, and a linear approximation for the temperature gradient in the heat exchanger, the model of the CSTR-external heat exchanger network becomes:

$$
\begin{aligned}
\dot{M} &= F_o - F \\
\dot{\underline{C}} &= \underline{\underline{S}}\underline{r} + \frac{F_o}{M}(\underline{C_o} - \underline{C}) \\
\dot{T} &= -\frac{1}{C_p}\underline{\Delta H}^T\underline{r} + \frac{F_o}{M}(T_o - T) + \frac{R}{M}(T_R - T) \\
\dot{T}_R &= \frac{R}{M_R}(T - T_R) - \frac{UA}{C_p M_R}(T_R - T_C) \\
\dot{T}_C &= \frac{Fc}{M_C}(T_{Co} - T_C) + \frac{UA}{C_{pc}M_C}(T_R - T_C)
\end{aligned}
\tag{1}
$$

where U denotes the overall heat transfer coefficient in the heat exchanger and A the heat transfer area.

Let us now define:

$$
\varepsilon = \frac{F_{os}}{R_s} \tag{2}
$$

where the subscript s denotes steady-state values. Since the recycle flowrate R_s is much larger than the reactor feed F_{os}, $\varepsilon \ll 1$. Also, we define the scaled (potentially manipulated) inputs $u_o = F_o/F_{os}$, $u_F = F/F_s$, $u_R = R/R_s$ and $u_c = F_c/F_{cs}$, and the $\mathcal{O}(1)$ quantity $k_f = F_s/F_{os}$.

The model of Eq. 1 thus becomes:

$$
\begin{aligned}
\dot{M} &= F_{os}(u_o - k_F u_f) \\
\dot{\underline{C}} &= \underline{\underline{S}}\underline{r} + \frac{F_{os}}{M}u_o(\underline{C_o} - \underline{C}) \\
\dot{T} &= -\frac{1}{C_p}\underline{\Delta H}^T\underline{r} + \frac{F_{os}}{M}u_o(T_o - T) + \frac{1}{\varepsilon}\frac{F_{os}}{M}u_R(T_R - T) \\
\dot{T}_R &= \frac{1}{\varepsilon}\frac{F_{os}}{M_R}u_R(T - T_R) - \frac{UA}{C_p M_R}(T_R - T_C) \\
\dot{T}_C &= \frac{Fc}{M_C}(T_{Co} - T_C) + \frac{UA}{C_{pc}M_C}(T_R - T_C)
\end{aligned}
\tag{3}
$$

In practical applications, for useful energy removal or recovery, the flowrates of external cooling utility streams for the heat exchanger will be in direct relationship with the reaction mass throughput, *i.e.* a high recycle rate will require a high coolant flowrate. Hence, we can assume that $F_{cs}/R_s = k_r = \mathcal{O}(1)$ and consequently $F_s/F_{cs} = \mathcal{O}(\varepsilon)$. Also, we assume that $\frac{UA}{C_p M_C}$ is sufficiently large so that the cross–stream heat transfer rate in the heat exchanger is of the same order of magnitude as the net rate at which heat is input to the heat exchanger by the recycle stream R:

$$
\frac{(UA(T_R - T_C))_s}{(RC_p(T - T_R))_s} = \mathcal{O}(1)
$$

or, that the time constants for heat transfer and mass transport are of the same order of magnitude, *i.e.*

$$
\frac{\frac{UA}{C_p M_R}}{\frac{R_s}{M_R}} = k_h = \mathcal{O}(1)
$$

or, using Eq. 2,

$$
\frac{UA}{C_p M_R} = k_h \frac{F_{os}}{\varepsilon M_R}
$$

With the above notation, the dynamic model of the process network in Fig. 1 can be written as:

$$
\begin{aligned}
\dot{M} &= F_{os}(u_o - k_F u_f) \\
\dot{\underline{C}} &= \underline{\underline{S}}\underline{r} + \frac{F_{os}}{M}u_o(\underline{C_o} - \underline{C}) \\
\dot{T} &= -\frac{1}{C_p}\underline{\Delta H}^T\underline{r} + \frac{F_{os}}{M}u_o(T_o - T) + \frac{1}{\varepsilon}\frac{F_{os}}{M}u_R(T_R - T) \\
\dot{T}_R &= \frac{1}{\varepsilon}\frac{F_{os}}{M_R}u_R(T - T_R) - \frac{1}{\varepsilon}\frac{k_h F_{os}}{M_R}(T_R - T_C) \\
\dot{T}_C &= \frac{1}{\varepsilon}\frac{k_r F_{os}}{M_C}u_c(T_{Co} - T_C) + \frac{1}{\varepsilon}\frac{k_h k_{cp} F_{os}}{M_C}(T_R - T_C)
\end{aligned}
\tag{4}
$$

Due to the presence of flowrates of different magnitudes and of fast heat transfer, the above model is stiff, its stiffness being captured by the small singular perturbation parameter ε.

In the following section we show, via a singular perturbation analysis, that the dynamics of the network (1) exhibits two time scales, and obtain non–stiff, reduced–order models of the dynamics in each time scale.

2.2 *Model reduction and Control*

We proceed with our analysis starting from the fast time scale. To this end, we define the "stretched", fast time scale $\tau = t/\varepsilon$ in which Eq. 4 becomes:

$$\begin{aligned}
\frac{dM}{d\tau} &= \varepsilon F_{os}(u_o - k_F u_f) \\
\frac{d\underline{C}}{d\tau} &= \varepsilon \left[\underline{\underline{S}}\underline{r} + \frac{F_{os}}{M} u_o(\underline{C_o} - \underline{C}) \right] \\
\frac{dT}{d\tau} &= -\varepsilon \left[\frac{1}{C_p} \underline{\Delta H}^T \underline{r} + \frac{F_{os}}{M} u_o(T_o - T) \right] + \\
&\quad \frac{F_{os}}{M} u_R(T_R - T) \\
\frac{T_R}{d\tau} &= \frac{F_{os}}{M_R} u_R(T - T_R) - \frac{k_h F_{os}}{M_R}(T_R - T_C) \\
\frac{T_C}{d\tau} &= \frac{k_r F_{os}}{M_C} u_c(T_{Co} - T_C) + \frac{k_h k_{cp} F_{os}}{M_C}(T_R - T_C)
\end{aligned} \tag{5}$$

Then, we consider the limit $\varepsilon \to 0$, corresponding to infinitely large recycle and cooling medium flowrates and infinitely fast heat transfer in the heat exchanger. In this limit, we obtain the following description of the process network dynamics in the fast time scale:

$$\begin{aligned}
\frac{dT}{d\tau} &= \frac{F_{os}}{M} u_R(T_R - T) \\
\frac{T_R}{d\tau} &= \frac{F_{os}}{M_R} u_R(T - T_R) - \frac{k_h F_{os}}{M_R}(T_R - T_C) \\
\frac{T_C}{d\tau} &= \frac{k_r F_{os}}{M_C} u_c(T_{Co} - T_C) + \frac{k_h k_{cp} F_{os}}{M_C}(T_R - T_C)
\end{aligned} \tag{6}$$

Notice that the large recycle and coolant flowrates u_R and u_C are the only manipulated inputs available in this fast time scale, and can be used to address temperature stabilization and regulation objectives.

Turning to the slow dynamics, multiplying Eq. 4 by ε and considering the limit $\varepsilon \to 0$, we obtain the following quasi-steady state constraints:

$$\begin{aligned}
0 &= \frac{F_{os}}{M} u_R(T_R - T) \\
0 &= \frac{F_{os}}{M_R} u_R(T - T_R) - \frac{k_h F_{os}}{M_R}(T_R - T_C) \\
0 &= \frac{k_r F_{os}}{M_C} u_c(T_{Co} - T_C) + \frac{k_h k_{cp} F_{os}}{M_C}(T_R - T_C)
\end{aligned} \tag{7}$$

or, equivalently,

$$\begin{aligned}
0 &= T_R - T \\
0 &= T_R - T_C \\
0 &= T_{Co} - T_C
\end{aligned} \tag{8}$$

The constraints in Eq. 8 are linearly independent and hence they can be solved for the quasi-steady state values $\underline{\Theta}^\star = [T^\star, T_R^\star, T_C^\star]$ of the variables $\underline{\Theta} = [T, T_R, T_C]$, *i.e.*

$$T^\star = T_R^\star = T_C^\star = T_{Co}$$

Substituting the value for $T^\star$, we then obtain:

$$\begin{aligned}
\dot{M} &= F_s(k_f u_o - u_F) \\
\dot{\underline{C}} &= \underline{\underline{S}}\underline{r}(T^\star) + \frac{k_f F_s}{M} u_o(\underline{C_o} - \underline{C})
\end{aligned} \tag{9}$$

which represents the model of the slow dynamics of the process network. Note that only the small feed and effluent flowrates u_o and u_F are available as manipulated inputs in this slow time scale.

Remark 1. Due to the independence of the constraints (8), the system in Eq. 5 is in a *standard* singularly perturbed form (Kumar and Daoutidis, 1999), whereby one can distinguish between the fast variables $\underline{\Theta}$ (Eq. 6), and the slow ones, M and $\underline{C}$ (Eq. 9). Equivalently, the energy-related variables and the variables in the material balance of the process network in Figure 1 evolve in different time scales, with the former being faster than the latter.

Remark 2. Notice that the rates of heat generation from the $\mathcal{R}$ reactions are the product of two terms, ΔH_i and r_i, corresponding to the heat of reaction and reaction rate, respectively. Consequently, a high rate of heat generation by reaction could occur both in reacting systems in which fast reactions with moderate reaction enthalpies are present, and in reacting systems in which the reactions have moderate rates and a high heat of reaction. In the former case, the material balance of Eq. 9 will itself be in a nonstandard singularly perturbed form (Vora and Daoutidis, 2001), and further reduction steps will be necessary in order to obtain non-stiff descriptions of the intermediate and slow dynamics.

Remark 3. The analysis framework we presented is also applicable if an inert component is used as a heat carrier. In this case, the the model (1) would be augmented by the equations corresponding to the model of the separation unit. However, the stoichiometric matrix $\underline{\underline{S}}$ and and reaction rates $\underline{r}$ would remained unchanged, as the inert component does not partake in any reaction.

Remark 4. The arguments presented above indicate that the control objectives related to the energy-balance related fast variables T and T_R should be addressed using the large flowrates u_R and u_C, whereas the control objectives involving the slow variables in the material balance (such as the reactor holdup and product purity or distribution) should be addressed using u_o and u_F.

2.3 *Illustrative example*

Consider the process network in Fig. 2. It comprises of a CSTR, of volume M connected to an external heat exchanger by a recycle stream R. Two parallel

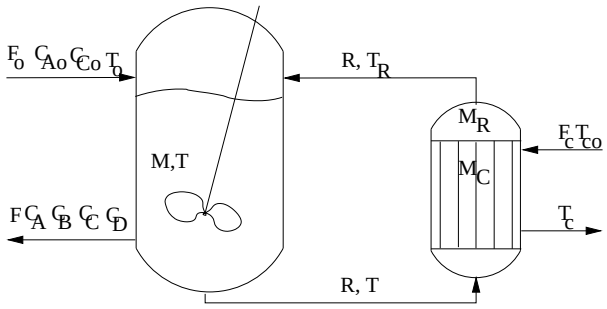

Fig. 2. CSTR with external heat exchanger

reactions take place in the reactor:

$$A \xrightarrow{k_1} 2B \tag{10}$$

$$B + C \xrightarrow{k_2} D \tag{11}$$

The feed stream F_o contains the reactants A and C and its composition C_{Ao}, C_{Co} is assumed to be constant. The intermediate B and the product D, as well as the unreacted A and C are removed at a rate F. We assume that the amount of heat generated in the two reactions is high, and that the reactor cannot be run adiabatically. In order to control the reactor temperature and prevent reaction runaway, the reaction mass is recycled through the tube side of the heat exchanger, at a (constant) high rate R. The coolant, of heat capacity C_{pc}, initially at temperature T_{co} is circulated though the heat exchanger shell at a rate F_c. The holdups in the heat exchanger shell and tube sides, respectively M_R and M_C are considered to be constant. We denote the heat transfer coefficient in the heat exchanger by U and let A be the transfer area. All units are modeled as lumped parameter systems, with a linear approximation for the temperature gradient in the heat exchanger.

The objectives for this process are control of the reactor temperature T, together with the control of the total holdup of the network (in this case, equivalent to the control of the reactor holdup M) and the product purity C_D.

With the assumptions stated above, the model of the process in Fig. 2 has the following form:

$$\begin{aligned}
\dot{M} &= F_0 - F \\
\dot{C}_A &= \frac{F_o}{M}(C_{Ao} - C_A) - k_{10}e^{-\frac{Ea_1}{RT}}C_A \\
\dot{C}_B &= -\frac{F_o}{M}C_B + 2k_{10}e^{-\frac{Ea_1}{RT}}C_A - k_{20}e^{-\frac{Ea_2}{RT}}C_BC_C \\
\dot{C}_C &= \frac{F_o}{M}(C_{Co} - C_C) - k_{20}e^{-\frac{Ea_2}{RT}}C_BC_C \\
\dot{C}_D &= -\frac{F_o}{M}C_D + k_{20}e^{-\frac{Ea_2}{RT}}C_BC_C \\
\dot{T} &= \frac{F_o}{M}(T_o - T) + \frac{R}{M}(T_R - T) \\
&\quad -\frac{\Delta H_1}{C_p}k_{10}e^{-\frac{Ea_1}{RT}}C_A \\
&\quad -\frac{\Delta H_2}{C_p}k_{20}e^{-\frac{Ea_2}{RT}}C_BC_C \\
\dot{T}_R &= \frac{R}{M_R}(T - T_R) - \frac{UA}{C_pM_R}(T_R - T_C) \\
\dot{T}_c &= \frac{Fc}{M_C}(T_{Co} - T_C) + \frac{UA}{C_{pc}M_C}(T_R - T_C)
\end{aligned} \tag{12}$$

which, by defining the small singular perturbation parameter

$$\varepsilon = \frac{F_{os}}{R_s}$$

the $\mathcal{O}(1)$ quantities

$$k_r = \frac{F_{cs}}{R_s}$$

$$k_f = \frac{F_s}{F_{os}}$$

$$k_{cp} = \frac{C_p}{C_{pc}}$$

$$k_h = \frac{UA}{R_sC_p}$$

and the manipulated inputs $u_o = F_o/F_{os}$, $u_F = F/F_s$, $u_R = R/R_s$ and $u_c = F_c/F_{cs}$, can be rewritten as:

$$\begin{aligned}
\dot{M} &= F_{os}(u_o - k_f u_F) \\
\dot{C}_A &= \frac{F_{os}}{M}u_o(C_{Ao} - C_A) - k_{10}e^{-\frac{Ea_1}{RT}}C_A \\
\dot{C}_B &= -\frac{F_{os}}{M}u_oC_B + 2k_{10}e^{-\frac{Ea_1}{RT}}C_A \\
&\quad -k_{20}e^{-\frac{Ea_2}{RT}}C_BC_C \\
\dot{C}_C &= \frac{F_{os}}{M}u_o(C_{Co} - C_C) - k_{20}e^{-\frac{Ea_2}{RT}}C_BC_C \\
\dot{C}_D &= -\frac{F_{os}}{M}u_oC_D + k_{20}e^{-\frac{Ea_2}{RT}}C_BC_C \\
\dot{T} &= \frac{F_{os}}{M}u_o(T_o - T) + \frac{1}{\varepsilon}\frac{F_{os}}{M}u_R(T_R - T)
\end{aligned} \tag{13}$$

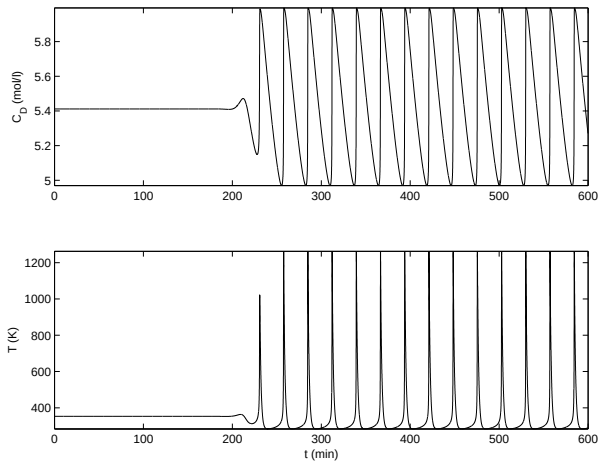

Fig. 3. Oscillatory open loop behavior of the reactor-external feed exchanger network (12). Temperature control is switched off at $t = 100$ min

$$-\frac{\Delta H_1}{C_p} k_{10} e^{-\frac{Ea_1}{RT}} C_A$$

$$-\frac{\Delta H_2}{C_p} k_{20} e^{-\frac{Ea_2}{RT}} C_B C_C$$

$$\dot{T}_R = \frac{1}{\varepsilon}\frac{F_{os}}{M_R} u_R (T - T_R) - \frac{1}{\varepsilon}\frac{k_h F_{os}}{M_R}(T_R - T_C)$$

$$\dot{T}_C = \frac{1}{\varepsilon}\frac{k_r F_{os}}{M_C} u_c (T_{Co} - T_C) + \frac{1}{\varepsilon}\frac{k_h k_{cp} F_s}{M_C}(T_R - T_C)$$

We now apply the model reduction framework outlined in Section 2.2. In order to obtain a description of the fast dynamics, we define the fast time scale $\tau = t/\varepsilon$, and, in the limit of the recycle and coolant flow rate and the heat transfer coefficient in the heat exchanger becoming infinite *i.e.* $\varepsilon \to 0$, we obtain a description of the fast dynamics of the reactor-heat exchanger process network (13):

$$\frac{dT}{d\tau} = \frac{F_{os}}{M} u_R (T_R - T) \tag{14}$$

$$\frac{dT_R}{d\tau} = \frac{F_{os}}{M_R} u_R (T - T_R) - \frac{k_h F_{os}}{M_R}(T_R - T_C)$$

$$\frac{dT_c}{d\tau} = \frac{k_r F_{os}}{M_C} u_c (T_{Co} - T_C) + \frac{k_h k_{cp} F_s}{M_C}(T_R - T_C)$$

According to the analysis in Section 2.2, we address the control of the reactor temperature T in the fast time scale, using the large flowrate u_C as a manipulated input, and the proportional feedback law:

$$u_C = 1 + K_C (T - T_{sp}) \tag{15}$$

Eq. (14) yields the quasi–steady state value $T^\star = T_{Co}$. Substituting $T^\star$ in Eq. 13, we obtain a description of the slow dynamics of the reactor-heat exchanger network:

$$\dot{M} = F_o - F \tag{16}$$

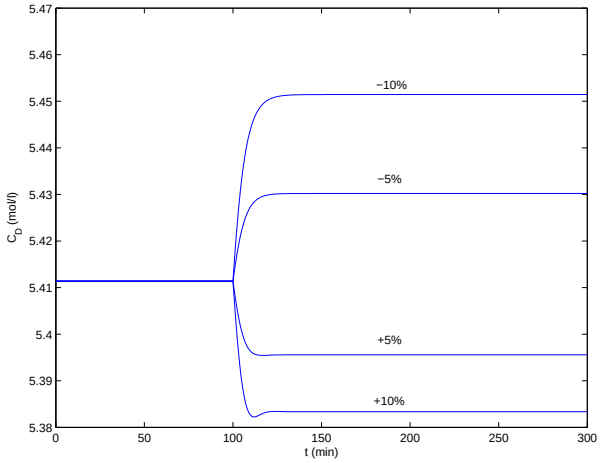

Fig. 4. Nonlinear behavior of the slow dynamics of the reactor-external heat exchanger network: change in C_D for different step changes in the feed flowrate F_o, from the nominal value F_{os}

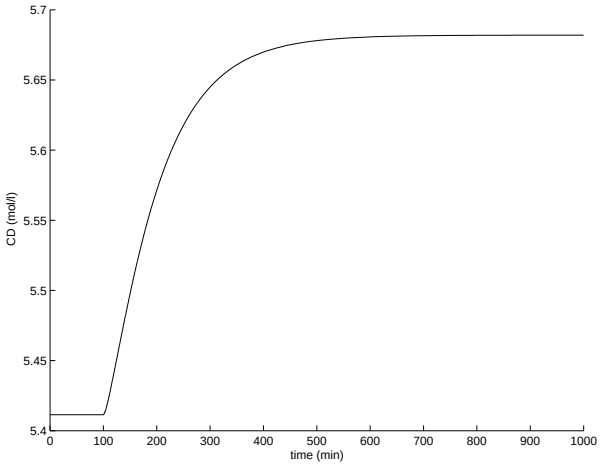

Fig. 5. Closed loop evolution of the product purity

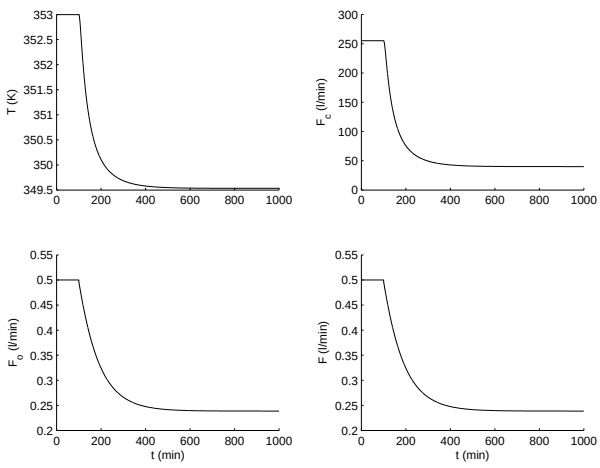

Fig. 6. Closed loop evolution of the reactor temperature and of the feed, product and coolant flowrates

$$\dot{C}_A = \frac{F_o}{M}(C_{A0} - C_A) - k_{10} e^{-\frac{Ea_1}{RT_{Co}}} C_A$$

$$\dot{C}_B = -\frac{F_o}{M}C_B + 2k_{10}e^{-\frac{Ea_1}{RT_{Co}}}C_A - k_{20}e^{-\frac{Ea_2}{RT_{Co}}}C_BC_C$$
$$\dot{C}_C = \frac{F_o}{M}(C_{C0} - C_C) - k_{20}e^{-\frac{Ea_2}{RT_{Co}}}C_BC_C$$
$$\dot{C}_D = -\frac{F_o}{M}C_D + k_{20}e^{-\frac{Ea_2}{RT_{Co}}}C_BC_C$$

We carried out numerical simulations, using the nominal values in Table 1. Initially, we simulated the system switching the temperature controller (15) off at $t = 100$ min, and recording the subsequent behavior. Without temperature control, the behavior of the reactor-heat exchanger network is oscillatory (Fig. 3), with very large deviations in the reactor temperature T. In the simulation presented in Fig. 3, the proportional controller in Eq. 15 (with $K_C = 0.9$) stabilizes the fast dynamics of the network.

According to the analysis in Section 2.2, after setting the reactor temperature with the control law (14), the control of the total holdup M and of the product purity C_D should be addressed in the slow time scale using the small flowrates F_0 and F. Figure 4 shows the profiles for the product purity C_D for different step changes in F_0, in the system with the proportional controller of Eq. 14. The responses indicate a nonlinear behavior of the slow dynamics of the reactor-external heat exchanger network.

Based on the reduced order model (16) we designed a multivariable input–output linearizing feedback controller with integral action (Daoutidis and Kravaris, 1994) for the product purity and for the total holdup (that acts as an integrator), using respectively u_o and u_F as manipulated inputs, requesting a first–order decoupled response:

$$C_D + \beta_1 \frac{dC_D}{dt} = C_{D,sp} \qquad (17)$$
$$M + \beta_2 \frac{dM}{dt} = M_{sp}$$

with $\beta_1 = 30$ min and $\beta_2 = 30$ min.

Figures 5–6 present the closed–loop behavior of the reactor–heat exchanger system for a 5% increase in the product purity setpoint at $t = 100$ min in the nominal case. Clearly, the proposed controller yields the desired performance, imposing the requested first–order response. Figures 5–6 show the corresponding profiles in the case of a modeling error (a -16% error in the heat transfer coefficient U and a $+5K$ unmeasured disturbance in the coolant initial temperature T_{Co}). The controller performance is very robust with respect to these disturbances.

3. DYNAMICS OF HIGH PURITY DISTILLATION COLUMNS

High purity distillation columns rely on a high internal recycle for increasing the purity of the

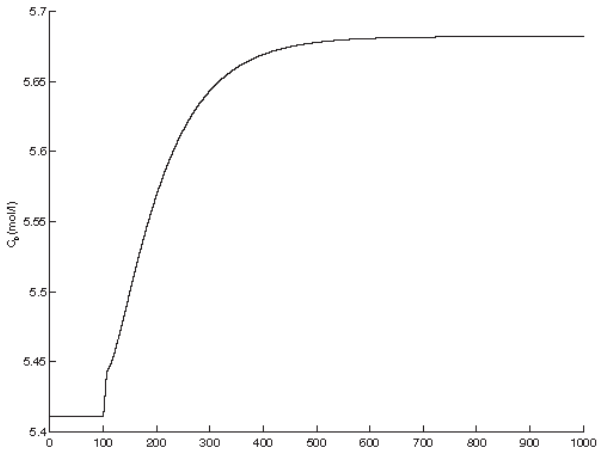

Fig. 7. Closed loop evolution of the product purity in the presence of modeling errors

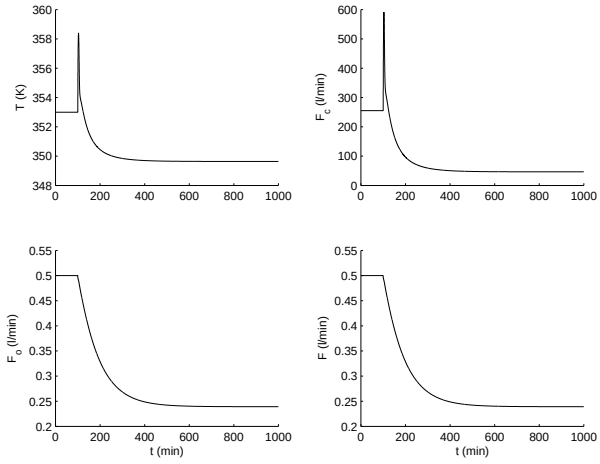

Fig. 8. Closed loop evolution of the reactor temperature and of the feed, product and coolant flowrates in the presence of modeling errors

distillate/bottoms streams. In our previous work (Kumar and Daoutidis, 2003), we have provided a rigorous justification of the two time scale behavior exhibited by such columns, and developed an explicit nonlinear low-order model of the slow input/output dynamics that is suitable for analysis and controller design. In the present work, we analyze the energy dynamics of high purity distillation columns. Using singular perturbation arguments, we show that the

Table 1. Nominal values for the process parameters

F_0	0.5 l/min	T_o	298 K
F	0.5 l/min	T_{co}	278 K
R	60 l/min	T	353 K
F_C	255.1 l/min	T_R	296 K
M	50 l	k_{10}	129.32 min^{-1}
M_R	40 l	k_{20}	70.50 $l/(mol\ min)$
M_C	40 l	ΔH_1	-92000 J/mol
C_{A0}	3 mol/l	ΔH_2	-229000 J/mol
C_{C0}	10 mol/l	Ea_1	20300 J/mol
UA	120000 $JK^{-1}min^{-1}$	Ea_2	30000 J/mol
K_C	0.9	Cp_c	229.9 $Jl^{-1}K^{-1}$
		Cp	220 $Jl^{-1}K^{-1}$

presence of the large internal flowrates leads to a high energy *throughput* (compared to the energy content of the product streams) and that the energy dynamics of the column evolves in the fast time scale.

3.1 *Modeling of a high purity distillation column*

We consider a distillation column with N trays (numbered from top to bottom), to which a saturated liquid containing a mixture of three components with mole fractions x_{1f}, x_{2f} of components 1 and 2 respectively, is fed at (molar) flowrate F_0 on tray N_f. The heavy component 3 which is the desired product is removed at the bottom from the reboiler at a flowrate B, while the lighter components 1 and 2 are removed at the top from the condenser at a flowrate D. In this column, large (compared to the feed, distillate and bottom product flowrates) vapor boilup V_B and liquid recycle R are used to attain a high purity of the desired component 3 in the bottom product. For simplicity, we model the heat transfer in the reboiler and condenser by using heat duties and denote by Q_R and Q_C the heat duties in the reboiler and the condenser, respectively. We assume that the relative volatilities of the three components are constant, and hence, that the phase equilibrium relationships are given by :

$$y_{1,i} = \frac{\alpha_1 x_{1,i}}{1 + (\alpha_1 - 1)x_{1,i} + (\alpha_3 - 1)x_{3,i}} \qquad (18)$$
$$y_{3,i} = \frac{\alpha_3 x_{3,i}}{1 + (\alpha_1 - 1)x_{3,i} + (\alpha_3 - 1)x_{3,i}}$$

We consider that the heat capacities $C_{p,l}$ and $C_{p,v}$ of the liquid and vapor phases are constant. Under the above assumptions, a standard dynamic model of the column is obtained:

$$\dot{M_C} = V_B - R - D \qquad (19)$$

$$\dot{x}_{1,D} = \frac{V_B}{M_C}(y_{1,1} - x_{1,D})$$

$$\dot{x}_{3,D} = \frac{V_B}{M_C}(y_{3,1} - x_{3,D})$$

$$\dot{T_C} = \frac{1}{M_C C_{p,l}}[V_B(Cp_V T_1 + \sum_{j=1}^{3} y_{j,1}\lambda_j - C_{p,l}T_C) - Q_C]$$

$$\vdots$$

$$\dot{x}_{1,i} = \frac{1}{M_i}[V_B(y_{1,i+1} - y_{1,i}) + R(x_{1,i-1} - x_{1,i})]$$

$$\dot{x}_{3,i} = \frac{1}{M_i}[V_B(y_{3,i+1} - y_{3,i}) + R(x_{3,i-1} - x_{3,i})]$$

$$\vdots$$

$$\dot{x}_{1,N_f} = \frac{1}{M_{N_f}}[V_B(y_{1,N_f+1} - y_{1,N_f}) + R(x_{1,N_f-1} - x_{1,N_f}) + F(x_{1,N_f-1} - x_{1,N_f})]$$

$$\dot{x}_{3,N_f} = \frac{1}{M_{N_f}}[V_B(y_{3,N_f+1} - y_{3,N_f}) + R(x_{3,N_f-1} - x_{3,N_f}) + F(x_{3,N_f-1} - x_{3,N_f})]$$

$$\vdots$$

$$\dot{x}_{1,i} = \frac{1}{M_i}[V_B(y_{1,i+1} - y_{1,i}) + R(x_{1,i-1} - x_{1,i}) + F(x_{1,i-1} - x_{1,i})]$$

$$\dot{x}_{3,i} = \frac{1}{M_i}[V_B(y_{3,i+1} - y_{3,i}) + R(x_{3,i-1} - x_{3,i}) + F(x_{3,i-1} - x_{3,i})]$$

$$\vdots$$

$$\dot{M}_R = R - V_B + F - B$$

$$\dot{x}_{1,B} = \frac{1}{M_R}[R(x_{1,N} - x_{1,B}) - V_B(y_{1,B} - x_{1,B}) + F(x_{1,N} - x_{1,B})]$$

$$\dot{x}_{3,B} = \frac{1}{M_R}[R(x_{3,N} - x_{3,B}) - V_B(y_{3,B} - x_{3,B}) + F(x_{3,N} - x_{3,B})]$$

$$\dot{T_R} = \frac{1}{M_R C_{p,l}}[RC_{p,l}(T_n - T_R) + FC_{p,l}(T_n - T_R) - V_B(C_{p,v} - C_{p,l})T_R - V_B\sum_{j=1}^{3} y_{j,B}\lambda_j + Q_B]$$

In Eq. 19, $M_C, x_{1,D}, x_{3,D}, y_{1,D}, y_{3,D}$ and T_D are the molar liquid holdup, liquid mole fractions, vapor mole fractions of components 1 and 3 and the temperature in the condenser, $M_i, x_{1,i}, x_{3,i}, y_{1,i}, y_{3,i}$ and T_i are the molar liquid holdup, liquid mole fractions, vapor mole fractions of components 1 and 3 and (constant) temperature on tray i and $M_R, x_{1,B}, x_{3,B}, y_{1,B}$, $y_{3,B}$ and T_R are the corresponding holdup, liquid mole fractions, vapor mole fractions and temperature in the reboiler.

3.2 *Model reduction*

In the case of the high purity distillation column, the presence of a large liquid recycle R implies an equally large liquid boilup V_B at the nominal steady state. On the other hand, the feed flow rate F, the distillate flow rate F and the bottom product flow rate B are of the same order of magnitude. Therefore, we can define $\varepsilon = (D_s/R_s) \ll 1$ and $k_1 = V_{B,s}/R_s = \mathcal{O}(1)$, where the subscript s refers to the nominal steady state.

Note that the energy content of the large internal flowrates R and V_B is much larger than that of the feed, distillate and bottom product, *i.e.* :

$$\frac{(DC_{p,l}T_C)_s}{(RC_{p,l}T_C)_s} \triangleq \frac{H_{Ds}}{H_{Rs}} = \varepsilon \qquad (20)$$

and, similarly, $H_{Ds}/H_{V_Bs} = \mathcal{O}(\varepsilon)$. In order to obtain a large vapor boilup V_B, the nominal heat duty of the reboiler $Q_{R,s}$ will be equally large, *i.e.* $Q_{Rs}/H_{V_Bs} = \mathcal{O}(1)$ and, consequently, $H_{Ds}/Q_{Rs} = \varepsilon/k_R$, where $k_R = \mathcal{O}(1)$. Note also that Q_C and Q_R will be of comparable magnitude, as a large condenser heat duty is required when a large vapor boilup is present. Hence, we can write $H_{Ds}/Q_{Cs} = \varepsilon/k_C$, $k_C = \mathcal{O}(1)$.

With the above notation, the model of the high purity distillation column can be rewritten in the form:

$$\dot{M}_C = \frac{D_s}{\varepsilon}(\bar{V}_B - \bar{R}) - D \tag{21}$$

$$\dot{x}_{1,D} = \frac{D_s k_1 \bar{V}_B}{\varepsilon M_C}(y_{1,1} - x_{1,D})$$

$$\dot{x}_{3,D} = \frac{D_s k_1 \bar{V}_B}{\varepsilon M_C}(y_{3,1} - x_{3,D})$$

$$\dot{T_C} = \frac{D_s}{\varepsilon M_C C_{p,l}}[k_1 \bar{V}_B(Cp_V T_1 + \sum_{j=1}^{3} y_{j,1}\lambda_j - C_{p,l}T_C) - k_C \frac{H_{Ds}}{D_s}\bar{Q}_C]$$

$$\vdots$$

$$\dot{x}_{1,i} = \frac{D_s}{\varepsilon M_i}[k_1 \bar{V}_B(y_{1,i+1} - y_{1,i}) + \bar{R}(x_{1,i-1} - x_{1,i})]$$

$$\dot{x}_{3,i} = \frac{D_s}{\varepsilon M_i}[k_1 \bar{V}_B(y_{3,i+1} - y_{3,i}) + \bar{R}(x_{3,i-1} - x_{3,i})]$$

$$\vdots$$

$$\dot{x}_{1,N_f} = \frac{D_s}{\varepsilon M_{N_f}}[k_1 \bar{V}_B(y_{1,N_f+1} - y_{1,i}) + \bar{R}(x_{1,N_f-1} - x_{1,N_f})] + \frac{F}{M_{N_f}}(x_{1,N_f-1} - x_{1,N_f})$$

$$\dot{x}_{3,N_f} = \frac{D_s}{\varepsilon M_{N_f}}[k_1 \bar{V}_B(y_{3,N_f+1} - y_{3,N_f}) + \bar{R}(x_{3,N_f-1} - x_{3,N_f})] + \frac{F}{M_{N_f}}(x_{3,N_f-1} - x_{3,N_f})]$$

$$\vdots$$

$$\dot{x}_{1,i} = \frac{D_s}{\varepsilon M_i}[k_1 \bar{V}_B(y_{1,i+1} - y_{1,i}) + \bar{R}(x_{1,i-1} - x_{1,i})] + \frac{F}{M_i}(x_{1,i-1} - x_{1,i})$$

$$\dot{x}_{3,i} = \frac{D_s}{\varepsilon M_i}[k_1 \bar{V}_B(y_{3,i+1} - y_{3,i}) + \bar{R}(x_{3,i-1} - x_{3,i})] + \frac{F}{M_i}(x_{3,i-1} - x_{3,i})]$$

$$\vdots$$

$$\dot{M}_R = \frac{D_s}{\varepsilon}(\bar{R} - k_1 \bar{V}_B) + F - B$$

$$\dot{x}_{1,B} = \frac{D_s}{\varepsilon M_R}[\bar{R}(x_{1,N} - x_{1,B}) - k_1 \bar{V}_B(y_{1,B} - x_{1,B})] + \frac{F}{M_R}(x_{1,N} - x_{1,B})$$

$$\dot{x}_{3,B} = \frac{D_s}{\varepsilon M_R}[\bar{R}(x_{3,N} - x_{3,B}) - k_1 \bar{V}_B(y_{3,B} - x_{3,B})] + \frac{F}{M_R}(x_{3,N} - x_{3,B})]$$

$$\dot{T_R} = \frac{D_s}{\varepsilon M_R C_{p,l}}[\bar{R}C_{p,l}(T_n - T_R) - k_1 \bar{V}_B((C_{p,v} - C_{p,l})T_R - \sum_{j=1}^{3} y_{j,B}\lambda_j) + k_B \frac{H_{Ds}}{D_s}\bar{Q}_B] + \frac{F}{M_R}C_{p,l}(T_n - T_R)$$

In the representation (21), $\bar{R}$, $\bar{Q}_C$ and $\bar{Q}_R$ denote scaled (and potentially manipulated) input variables:

$$\bar{R} = \frac{R}{R_s}, \;\; \bar{Q}_C = \frac{Q_C}{Q_{C,s}}, \;\; \bar{Q}_R = \frac{Q_R}{Q_{R,s}}$$

and

$$\bar{V}_B = \frac{V_B}{V_{B,s}}$$

Thus, the process model has the general form:

$$\dot{\underline{x}} = \underline{f}(\underline{x}) + \underline{\underline{g}}^s(\underline{x})\underline{u}^s + \underline{\underline{g}}^l(\underline{x})\underline{u}^l \tag{22}$$

where

$$x = [\chi \; \Theta]^T = [M_C \quad x_{1,D} \quad x_{3,D} \; \cdots \; x_{1,i} \quad x_{3,i} \; \cdots \quad M_R \quad x_{1,B} \quad x_{3,B} \quad T_C \; T_R]^T$$

is the vector of state variables ($\underline{\Theta} = [T_C \;\; T_R]^T$), $u^s = [D \;\; B]^T \in \mathbb{R}^2$ is the vector of manipulated inputs corresponding to small flowrates and $u^l = [\bar{R} \;\; \bar{Q}_C \;\; \bar{Q}_R]^T \in \mathbb{R}^3$ is the vector of manipulated inputs corresponding to large material and energy flows, while $\underline{f}(\underline{x})$ is a smooth vector field and $\underline{\underline{g}}^s(\underline{x})$ and $\underline{\underline{g}}^l(\underline{x})$ are smooth matrices. To account for the presence of both material and energy balance equations, we rewrite $\underline{\underline{g}}^l(\underline{x})$ as:

$$\underline{\underline{g}}^l(\underline{x}) = \begin{bmatrix} \underline{\underline{g}}^{lx}(\underline{x}) \\ \underline{\underline{g}}^{lt}(\underline{x}) \end{bmatrix} \tag{23}$$

with $\underline{\underline{g}}^{lx}(\underline{x}) \in \mathbb{R}^{(n-2)\times 3}$ and $\underline{\underline{g}}^{lt}(\underline{x}) \in \mathbb{R}^{(2)\times 3}$.

Note that the model (22) exhibits stiffness owing to the presence of the small parameter ε. In what follows, we analyze the time scale multiplicity induced by the model stiffness in the dynamic behavior of the high-purity column. We begin with a derivation of a description of the fast dynamics of the process. To this end, let us define the fast time scale $\tau = t/\varepsilon$. In this time scale, the system in Eq. 22, becomes:

$$\frac{d\underline{x}}{d\tau} = \varepsilon \underline{f}(\underline{x}) + \varepsilon \underline{\underline{g}}^s(\underline{x})\underline{u}^s + \underline{\underline{g}}^l(\underline{x})\underline{u}^l \tag{24}$$

Considering the limit $\varepsilon \to 0$, we obtain the following description of the fast dynamics of the system:

$$\frac{d\underline{x}}{d\tau} = \underline{\underline{g}}^{l}(\underline{x})\underline{u}^{l} \tag{25}$$

Note that the inputs $\underline{u}^{s}$ have no effect on the fast dynamics; only the inputs $\underline{u}^{l}$, corresponding to the large flow rates and large reboiler and condenser heat duties have an effect, and can be used for control in this fast time scale.

We now turn to the slow time scale t, in order to obtain a description of the slow dynamics. In particular, multiplying Eq. 22 by ε, and considering the limit $\varepsilon \to 0$, we obtain the following algebraic constraints, that need to be satisfied in the slow time scale:

$$\begin{bmatrix} -\bar{R} + k_1\bar{V}_B \\ k_1\bar{V}_B(y_{1,1} - x_{1,D}) \\ k_1\bar{V}_B(y_{3,1} - x_{3,D}) \\ \vdots \\ \bar{R}(x_{1,i-1} - x_{1,i}) + k_1\bar{V}_B(y_{1,i+1} - y_{1,i}) \\ \bar{R}(x_{3,i-1} - x_{3,i}) + k_1\bar{V}_B(y_{3,i+1} - y_{3,i}) \\ \vdots \\ \bar{R} - k_1\bar{V}_B \\ \bar{R}(x_{1,N} - x_{1,B}) - k_1\bar{V}_B(y_{1,B} - x_{1,B}) \\ \bar{R}(x_{3,N} - x_{3,B}) - k_1\bar{V}_B(y_{3,B} - x_{3,B}) \\ [k_1\bar{V}_B(Cp_V T_1 + \sum_{j=1}^{3} y_{j,1}\lambda_j - C_{p,l}T_C) - \\ k_C\bar{Q}_C\frac{H_{D_S}}{D_s}] \\ [\bar{R}(T_n - T_R) - \\ k_1\bar{V}_B\frac{((C_{p,v} - C_{p,l})T_R - \sum_{j=1}^{3} y_{j,B}\lambda_j)}{C_{p,l}} + \\ k_B\bar{Q}_R\frac{H_{D_S}}{D_s C_{p,l}}] \end{bmatrix} = \underline{0} \tag{26}$$

or, in a general form:

$$\begin{bmatrix} \underline{\underline{g}}^{lx}(\underline{x})\underline{u}^{l} \\ \underline{\underline{g}}^{lt}(\underline{x})\underline{u}^{l} \end{bmatrix} = \underline{0} \tag{27}$$

The constraints (26) denote the quasi-steady state condition for the fast dynamics described in Eq. 25. Once the large manipulated inputs $\bar{R}$, $\bar{Q}_C$ and $\bar{Q}_R$ are specified with appropriate control laws, the Jacobian matrix $\partial\underline{\underline{g}}^{lt}(\underline{x})\underline{u}^{l}/\partial\underline{\Theta}$, is non-singular, and hence the last two constraints can be solved for the quasi-steady state values $\underline{\Theta}^{\star} = [T_C^{\star}\ T_R^{\star}]^T$ of the condenser and reboiler temperatures. This implies that the temperatures $\underline{\Theta}$ only exhibit *fast* dynamics.

With the above observation, referring back to the system description in Eq. 22 and considering the limit $\varepsilon \to 0$ in the slow time scale t, it follows that the terms $\underline{\underline{g}}^{lx}(\underline{\chi}, \underline{\Theta}^{\star})\underline{u}^{l}/\varepsilon$ are indeterminate. Defining these finite, but unknown terms as the additional variables $\underline{z} = \lim_{\varepsilon\to 0} \underline{\underline{g}}^{lx}(\underline{\chi}, \underline{\Theta}^{\star})\underline{u}^{l}/\varepsilon$, we obtain a description (28) of the slow dynamics of the system of Eq. 22.

$$\begin{aligned} \dot{\underline{\chi}} &= \underline{f}(\underline{\chi}, \underline{\Theta}^{\star}) + \underline{\underline{g}}^{s}(\underline{\chi}, \underline{\Theta}^{\star}) + \underline{\underline{b}}(\underline{\chi}, \underline{\Theta}^{\star})\underline{z} \\ \underline{0} &= \underline{\underline{g}}^{lt}(\underline{x})\underline{u}^{l} \end{aligned} \tag{28}$$

where $\underline{\underline{b}}(\underline{\chi}, \underline{\Theta}^{\star})$ is the diagonal matrix:

$$\underline{\underline{b}}(\underline{\chi}, \underline{\Theta}^{\star}) = diag \begin{bmatrix} D_s \\ \frac{D_s}{M_C} \\ \frac{D_s}{M_C} \\ \vdots \\ \frac{D_s}{M_i} \\ \frac{D_s}{M_i} \\ \vdots \\ D_s \\ \frac{D_s}{M_R} \\ \frac{D_s}{M_R} \end{bmatrix} \tag{29}$$

Eq. (28) is a high-index differential algebraic equation (DAE) system, and the derivation of the corresponding ODE representation should be addressed using *e.g.* the methods presented in (Kumar and Daoutidis, 1999). Also, note that only the small flowrates $\underline{u}^{l}$ are present in the model (28), and are available (potentially in conjunction with the *set-points* of the fast controllers) for addressing control objectives in the slow time scale.

4. CONCLUSIONS

In this paper, we analyzed the energy dynamics of two prototype process networks with large recycle, a reactor with external heat exchanger and a high purity distillation column. In these networks, the large material recycle acts as an energy carrier, leading to a high energy throughput for the entire network. The presence of the large recycle stream causes stiffness in the network models, their dynamics exhibiting a time-scale separation. Using singular perturbation arguments, we showed that the variables in the energy balance of these networks evolve in the fast time scale, while the terms in the material balance equations can exhibit both fast and slow transients. Also within the framework of singular perturbations, we proposed a procedure for deriving reduced-order,

non-stiff models for the fast and slow dynamics, the latter typically of low order.

Furthermore, our approach allowed for a rational separation of the available material flow rates and/or heat duties into two distinct sets of manipulated inputs, that act and can be used to address control objectives in the two time scales. Specifically, the large flowrates and heat duties only act upon the fast dynamics, while the small ones act in the slow time scale.

Finally, the application of the proposed analysis and model reduction procedure was illustrated through numerical simulations in a reactor-external heat exchanger network example.

5. REFERENCES

Alhumaizi, K.L. (2000). Stability analysis of the ethylene dimerization reactor for the selective production of butene-1. Trans IChemE **78**, 492–498.

Baldea, M., P. Daoutidis and A. Kumar (2004). Dynamics of process networks with recycle and purge: time scale separation and model decomposition. In: Preprints of ADCHEM'03. Hong Kong. pp. 645–650.

Bildea, C.S. and A.C. Dimian (1998). Stability and multiplicity approach to the design of heat integrated PFR. AIChE J. **44**(12), 2703–2712.

Chen, Y.H. and C.C. Yu (2003). Design and control of heat integrated reactors. Ind. Eng. Chem. Res. **42**, 2791–2808.

Dadebo, S.A., M.L. Bell, P.J. McLellan and K.B. McAuley (1997). Temperature control of industrial gas phase polyethylene reactors. J. Proc. Contr. **7**(2), 83–95.

Daoutidis, P. and C. Kravaris (1994). Dynamic output feedback control of minimum-phase multivariable nonlinear processes. Chem. Eng. Sci. **49**, 433–447.

Farschman, C. A., K. P. Viswanath and B. E. Ydstie (1998). Process systems and inventory control. AIChE J. **44**(8), 1841–1857.

Georgakis, C (1986). On the use of extensive variables in process dynamics can control. Chem. Eng. Sci. **41**, 1471–1484.

Hangos, K. M., A. A. Alonso, J. D. Perkins and B. E. Ydstie (1999). Thermodynamic approach to the structural stability of process plants. AIChE J. **45**(4), 802–816.

Henderson, L.S. and R.A. Cornejo (1989). Temperature control of continuous, bulk styrene polymerization reactors and the influence of viscosity: An analytical study. Ind. Eng. Chem. Res. **28**, 1644–1653.

Jacobsen, E. and M. Berezowski (1998). Chaotic dynamics in homogeneous tubular reactors with recycle. Chem. Eng. Sci. **23**, 4023–4029.

Kothare, M. V., R. Shinnar, I. Rinard and M. Morari (2000). On defining the partial control problem: Concepts and examples. AIChE J. **46**, 2456–2474.

Kulhavy, R., J. Lu and T. Samad (2000). Emerging technologies for enterprise optimization in the process industries. In: Preprints of Chemical Process Control - 6. Tucson, Arizona. pp. 411–422.

Kumar, A. and P. Daoutidis (1999). Control of Nonlinear Differential Equation Systems. Vol. 397 of Research Notes in Mathematics Series. Chapman & Hall/CRC.

Kumar, A. and P. Daoutidis (2002). Dynamics and control of process networks with recycle. J. Proc. Contr. **12**, 475–484.

Kumar, A. and P. Daoutidis (2003). Nonlinear model reduction and control for high-purity distillation columns. IECres **42**, 4495–4505.

Luyben, M. L., B. D. Tyreus and W. L. Luyben (1997). Plantwide control design procedure. AIChE J. **43**(12), 3161–3174.

Luyben, W. L. (1993). Dynamics and control of recycle systems. parts 1-4.. Ind. Eng. Chem. Res. **32**, 466–486,1142–1162.

Luyben, W.L. (1998). External versus internal open-loop unstable processes. Ind. Eng. Chem. Res. **37**, 2713–2720.

Marquardt, W. (2000). Fundamental modeling and model reduction for optimization based control of transient processes. In: Preprints of Chemical Process Control - 6. Tucson, Arizona. pp. 30–60.

Mizsey, P and I. Kalmar (1996). Effects of recycle on control of chemical processes. Comput. chem. Engng. **20**, S883–S888.

Morud, J. and S. Skogestad (1994). Effects of recycle on dynamics and control of chemical processing plants. Comput. chem. Engng. **18**, S529–S534.

Ng, C. and G. Stephanopoulos (1998). Plant-wide control structures and strategies. In: Proc. of DYCOPS-5. Corfu, Greece. pp. 1–16.

Price, R. M. and C. Georgakis (1993). Plantwide regulatory control design procedure using a tiered framework. Ind. Eng. Chem. Res. **32**, 2693.

Reyes, F. and W.L. Luyben (2000). Steady-state and dynamic effects of design alternatives in heat-exchanger/ furnace/ reactor processes. Ind. Eng. Chem. Res. **39**, 3335–3346.

Seider, W.D., J.D. Seader and D.R. Lewin (1999). Process Design Principles. John Wiley and Sons, Inc.. New York.

Tyreus, B.D. (1999). Dominant variables for partial control. 1. A thermodynamic method for their identification. Ind. Eng. Chem. Res. **38**, 1432—1443.

Vora, N.P. and P. Daoutidis (2001). Nonlinear model reduction of chemical reaction systems. AIChE J. **47**, 2320–2332.

Yi, C. K. and W. L. Luyben (1997). Design and control of coupled reactor/column systems - parts 1-3.. Comput. chem. Engng. **21**(1), 25–68.